2018 IEEE Intelligent Vehicles Symposium (IV)
Changshu, Suzhou, China, June 26-30, 2018

Environment Modeling for the Application in Optimization-based Trajectory Planning

Christian Lienke[1], Martin Keller[2], Karl-Heinz Glander[2] and Torsten Bertram[1]

Abstract— **The paper at hand proposes an environment model for trajectory planning in structured environments. It is composed of a static and a dynamic environment model. The generated static potential field takes restrictions imposed by the static environment into account. The dynamic environment model is based on the physical interpretation of the required safety distance. By the use of an advanced obstacle trajectory prediction method, the safety distance is calculated in accordance to the predicted situation. As the safety distance affects the dynamic potential field, information provided by the obstacle trajectory prediction is directly considered in the ego vehicle trajectory planning process. On account of the predictive character of the developed environment potential field, simulation experiments demonstrate the feasibility and effectiveness of the proposed method.**

I. Introduction

In the architecture of modern vehicles the tasks of perception, planning and control play an important role. For comfortable and safe driving knowledge about the surrounding environment is a requirement. Based on the current situation and a future driving strategy a trajectory has to be planned, which is then realized by a subsequent vehicle dynamics controller. To plan a suitable trajectory for the current situation the information perceived by sensor data has to be transfered to the planning module. This is achieved via an environment model, which incorporates fused information about road geometry and obstacles like pedestrians or other vehicles.

A. Trajectory planning for automated driving

Trajectory planning approaches for automated driving can be divided into four distinct categories [1]: Incremental search, graph search, curve interpolation and numerical optimization methods. In previous work the authors presented a combination of curve interpolation and numerical optimization for efficient trajectory planning in structured environments [2], which can be categorized as a numerical optimization method. The major advantage of optimization based approaches is the ability to find the optimal solution for various maneuvers even in complex scenarios. Moreover, a major drawback of incremental and graph search methods is the significant increase of the computational burden with increasing dimension of the state space, while completeness can not be guaranteed for real-time applications. Despite the broad variety of optimization algorithms, hereinafter the term optimization-based is used synonymously for gradient-based.

[1]Christian Lienke and Torsten Bertram are with the Institute of Control Theory and Systems Engineering, TU Dortmund University, 44227 Dortmund, Germany, https://orcid.org/0000-0002-5952-9246 christian.goette@tu-dortmund.de

[2]Martin Keller and Karl-Heinz Glander are with Active & Passive Safety Technology, ZF Group, 40547 Düsseldorf, Germany

B. Environment modeling in trajectory planning approaches

In literature several approaches to environment modeling for collision avoidance in trajectory planning exist. In [2] obstacle vehicles are approximated by a circular shape obeying a predefined safety distance to take the spatial extent of the ego and obstacle vehicle into consideration. The static environment is modeled via the distance to the respective road boundary. The authors of [3] model the environment as polygons, wherein the static environment is imposed by the driving corridor. For moving objects the motion is predicted into the future to form a predefined polygon for every discrete time interval. All measures have in common that a left or right decision for the passing of other vehicles is determined a priori, which is then integrated into the shapes of the polygons, by extending them infinitely to one side of the space. In [4] obstacle vehicles are incorporated by adjusting the road boundaries utilizing two sigmoid functions. This prevents a local optimum between the obstacle and the road boundaries. Similarly [5] adjusts the forward collision avoidance constraint and the rear collision avoidance constraint in dependence on the driving lane of the obstacle, yielding a convex optimization problem. In the aforementioned cases environment models are tailored to the current situation and not suitable for a general solution as they adapt to the current situation by using logic or rigorously restrict the available free space, respectively. To gain a generic representation of the environment, as intended in this contribution, the desired behavior should not be included in the environment model.

A prevalent holistic representation of the environment is the use of occupancy grids, which are introduced by [6] for the application in the field of mobile robotics. Generally, 2D occupancy grids describe the static environment. Several subsequent approaches deal with the development of an extension for dynamic objects. The authors of [7] for example, present a grid-based tracking and mapping algorithm that simultaneously estimates the static and the dynamic environment. The disadvantages of occupancy grids can be seen in potential discretization errors and the presumably high memory consumption. Moreover, occupancy grids suffer from their representation as discrete cells with fixed sizes, such that they can be regarded as discontinuous and not appropriate for continuous optimization approaches. For this reason they can only be used for sampling based trajectory approaches like in [8].

978-1-5386-4451-5/18/$31.00 ©2018 IEEE

Another common representation of the environment is the potential field with high and low potentials for non negotiable and negotiable areas, respectively. In [9] a potential field within an integrated approach to collision avoidance and vehicle automation is introduced, which is composed of a static and a dynamic potential field. The authors of [10] present a driving safety field, which is divided in a potential field, a kinetic field and a behavior field. According to the authors the potential field corresponds to a static potential field denoting the influence of static objects on driving safety. The kinetic field on the other hand corresponds to the dynamic part of the environment, as it takes the influence of moving objects into consideration. Furthermore, the behavior field captures the influence of the driver behavior. The authors of [11] introduce a potential field hazard map for lane keeping (static) and collision avoidance (dynamic).

Starting from the developed trajectory planning approach in previous work [2] a holistic environment model suitable for optimization-based trajectory planning is given in this paper. In correspondence to existing representations of environment models (see e.g. [12]), the environment is separated in a static and a dynamic environment model. The static environment is provided as polynomial lane markers, whereas an obstacle list is chosen for dynamic obstacles. To gain a holistic description of the environment both representations are transformed to a potential field such that they can be combined to a comprehensive environment model suitable to perform the task of trajectory planning for automated driving. The aspect of the presented approach, which differs to existing approaches, is the fact that surrounding obstacles are taken into account via an advanced trajectory prediction based on [13]. In contrast to approaches with fixed safety distances derived from the current situation, the information provided by the obstacle trajectory prediction are directly considered in the ego trajectory planning process by affecting the dynamic potential field. The term fixed is herein defined w.r.t. time within the prediction horizon of the trajectory planning algorithm, meaning that safety distances are not changing over time during planning phase. To the best knowledge of the authors the predictive character represents a novel feature in comparison to other state of the art approaches, as the safety distance is calculated accordingly to the predicted situation in dependence on relative velocities and orientation. Thus the environment model beneficially adapts to the predicted future development of the current situation (cmp. Fig. 1).

The remainder of this paper is organized as follows. In section II the applied real-time capable trajectory planning approach is described in broad outline, focusing on the gradient-based formulation, which leads to the requirement of a differentiable environment model. The developed environment model is then presented in section III by defining the static and the dynamic potential field. In section IV the combined environment potential field is analyzed in connection with the optimization-based trajectory planning approach. Finally section V concludes the paper.

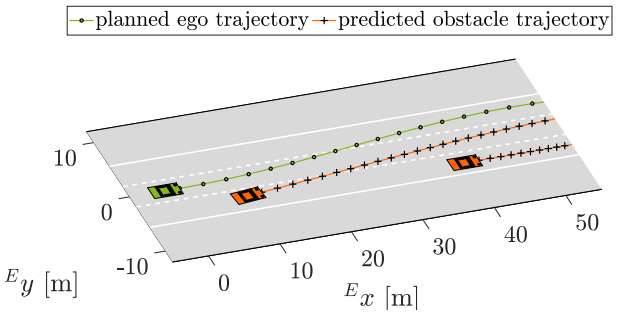

Fig. 1: Illustration of the predictive character of the environment model, as the dynamic potential field is build with the help of an advanced obstacle trajectory prediction approach.

II. Optimization-based Trajectory Planning

The idea of online trajectory optimization is based on the work of [14] from mobile robot applications. The developed real-time capable approach for trajectory planning in the context of automated driving enhances the approach by using a spline-based interpolation strategy [2].

In general the problem of trajectory optimization for a trajectory B can be formulated as a nonlinear program

$$\gamma^*(B, \mathbf{\Gamma_i}) = \min_B \sum_{i=1}^{z} \gamma_i(B, \mathbf{\Gamma_i}) \tag{1}$$

subject to

$$\begin{aligned} \mathbf{x}_1 &= \mathbf{x}_s, \\ \mathbf{f}_k(\mathbf{x}) &= \mathbf{0}, \\ \mathbf{h}_k(\mathbf{x}) &\leq \mathbf{0}, \end{aligned}$$

with actual state $\mathbf{x}_s$ and equality constraint $\mathbf{f}_k$ and inequality constraints $\mathbf{h}_k$ respectively. The goal state $\mathbf{x}_g$ is part of the optimization. There are z quadratic functions γ_i composed of objectives $\mathbf{o}_i$, which are weighted with matrix $\mathbf{\Gamma}_i$

$$\gamma_i(B, \mathbf{\Gamma}_i) = \mathbf{o}_i^{\mathrm{T}}(B)\mathbf{\Gamma}_i\mathbf{o}_i(B). \tag{2}$$

The solution to the nonlinear problem as formulated in equation (1) is given by means of the approximation of hard constraints. Therefore constraints $\mathbf{f}_k$ and $\mathbf{h}_k$ are transformed to penalty terms by using the concept of soft constraints. Thus an efficient real-time capable solution is gained. Equality constraints are not part of the optimization problem, due to the use of simplified vehicle dynamics description. Inequality constraints are replaced by

$$\chi(\mathbf{h}_k) = \max\{[\mathbf{0}, \mathbf{h}_k]\}. \tag{3}$$

Hence the total error vector $\mathbf{e}(B) : B \rightarrow \mathbb{R}^{d_{err}}$ is

$$\mathbf{e} = [\mathbf{o}_1, \mathbf{o}_2, \ldots \mathbf{o}_z, \chi(\mathbf{h}_1), \chi(\mathbf{h}_2), \ldots, \chi(\mathbf{h}_{n-1})]^{\mathrm{T}}. \tag{4}$$

The cost function can then be defined as

$$\Phi(\mathbf{b}, \mathbf{\Omega}) = \mathbf{e}(\mathbf{b})^{\mathrm{T}}\mathbf{\Omega}\mathbf{e}(\mathbf{b}), \tag{5}$$

with optimization vector $\mathbf{b}$ of dimension d_{opt} and weight matrix $\mathbf{\Omega} \in \mathbb{R}^{d_{err} \times d_{err}}$, which contains the weights for the respective objective in the sense of automated driving. The optimal solution for the transformed problem is given by

$$\mathbf{b}^* = \arg\min_{\mathbf{b}} \Phi(\mathbf{b}, \mathbf{\Omega}), \tag{6}$$

which leads to a nonlinear least-squares problem that is solved iteratively with the Levenberg-Marquardt algorithm ([15], [16]). After each successful Levenberg-Marquardt step the actual solution is updated by

$$\mathbf{b}^{+} = \mathbf{b} + \Delta\mathbf{b}. \tag{7}$$

The basic equation of the Levenberg-Marquardt algorithm is given as

$$(\mathbf{H} + \lambda_{LM}\mathbf{I})\Delta\mathbf{b} = \mathbf{g} \tag{8}$$

with damping factor λ_{LM}, identity matrix $\mathbf{I}$ and gradient

$$\mathbf{g} = \mathbf{J}^{\mathrm{T}}\mathbf{\Omega}\mathbf{e}(\mathbf{b}). \tag{9}$$

The Jacobian matrix $\mathbf{J} \in \mathbb{R}^{d_{err}\times d_{opt}}$ is further used to calculate an approximation of the Hessian matrix $\mathbf{H} \in \mathbb{R}^{d_{opt}\times d_{opt}}$ with

$$\mathbf{H} = \mathbf{J}^{\mathrm{T}}\mathbf{\Omega}\mathbf{J}. \tag{10}$$

From equations (9) and (10) the requirement of a differentiable environment model representation is derived. In the following the earth- and vehicle coordinate frame indicated by leading superscripts are denoted E and F, respectively. The prediction horizon is set to fixed T_p with constant time intervals $t \in [t_k \; t_{k+1}]$. With states $\mathbf{x}_k = [{}^{F}x_k, {}^{F}y_k]^{\mathrm{T}}$ and $k = 1 \dots n$ the ego vehicle trajectory is given as

$$\mathbf{x}_{ego} = [\mathbf{x}_1, t_1, \mathbf{x}_2, t_2, \dots, \mathbf{x}_k, t_k, \dots, \mathbf{x}_n, T_p]^{\mathrm{T}}. \tag{11}$$

For a further and more detailed description of the utilized trajectory planning approach the authors refer to [2].

III. Environment Modeling in Structured Environments

In this section the environment model suitable for gradient-based trajectory planning is described. A potential field is chosen as the representation of the environment in order to fulfill the requirement of a differentiable model. Both, the static and dynamic environment model are explained separately and then combined to a holistic environment model. For reasons of discussion and explanation, the characteristics of the developed static and dynamic potential field are illustrated at an example with three straight lanes and the ego and obstacle vehicle in the center lane of the road.

A. Static environment modeling

The static environment model can be seen as an extended driving corridor denoting the negotiable space i.e. the available lanes for the ego vehicle that allow to drive in the intended driving direction. There are at most three lanes considered, such that if present the available lanes are composed of the ego lane and the left and right neighboring lane. This does not represent a limitation in performance for scenarios with more than three lanes, as it is still sufficient information to enable the ego vehicle to perform complete basic maneuvers like lane changes and lane keeping. Note that furthermore obstacles included in the dynamic environment model will be predicted independently of the number of detected lanes. Information about the present lanes is obtained by on-board camera sensors, with the shape of each lane given as a third order polynomial for each lane marker. To generate the static potential field the model type of each lane marker is chosen dependent on the lane marker type, such that it distinguishes between lane makers which are allowed and not allowed to drive over. For the sake of convenience all lane marker types which do not allow the ego vehicle to pass are grouped and representatively denoted as solid lane markers, whereas all lane marker types, which are allowed to cross will be denoted as dashed lane markers. Lane markers are counted in ego vehicle coordinate frame F from the left to the right, starting with index $\ell = 0$ for the left lane marker of the left lane, index $\ell = 1$ for the left and index $\ell = 2$ for the right lane marker, as well as index $\ell = 3$ for the right lane marker of the right neighboring lane. The polynomial is evaluated for ${}^{F}x_k$ of each trajectory point and the distance to the road limit is approximated by the distance $\Delta\check{y}_k^{\ell}$ between the ${}^{F}y$-coordinates of the trajectory and the lane marker polynomials ℓ

$$\Delta\check{y}_k^{\ell=0} = +({}^{F}y_k - {}^{F}y_k^{\ell=0}), \tag{12a}$$
$$\Delta\check{y}_k^{\ell=1} = +({}^{F}y_k - {}^{F}y_k^{\ell=1}), \tag{12b}$$
$$\Delta\check{y}_k^{\ell=2} = -({}^{F}y_k - {}^{F}y_k^{\ell=2}), \tag{12c}$$
$$\Delta\check{y}_k^{\ell=3} = -({}^{F}y_k - {}^{F}y_k^{\ell=3}). \tag{12d}$$

In dependence on the lane marker type it is

$$\Delta y_k^{\ell} = \begin{cases} \Delta\check{y}_k^{\ell} & \text{for solid marker type} \\ -|\Delta\check{y}_k^{\ell}| & \text{for dashed marker type} \end{cases} \tag{13}$$

and with desired distance to the lane marker Λ_ℓ this yields

$$h_{\ell,k} = \Delta y_k^{\ell} + \Lambda_\ell. \tag{14}$$

The static potential field with costs Φ_S is generated from superposition of each $\chi(\mathbf{h}_\ell)$, using equation (3), equation (4) and equation (5). Therein $\mathbf{h}_\ell$ is the vectorized form of $h_{\ell,k}$. The resulting potential field for the static environment is depicted in Fig. 2.

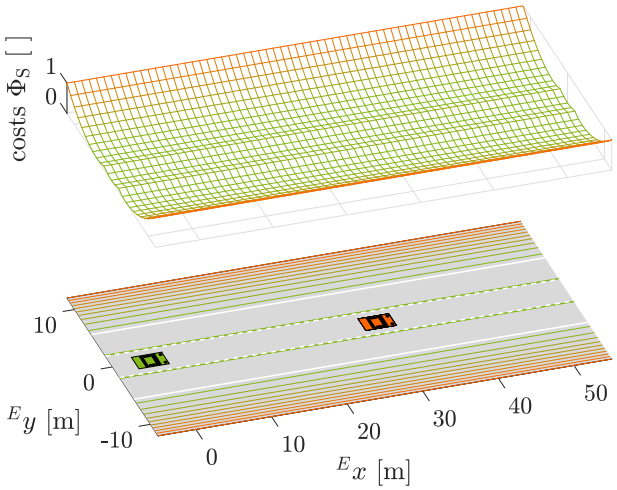

Fig. 2: Static potential field showing the two different models for solid and dashed lane marker types. For visualization purpose contour lines are projected on the road.

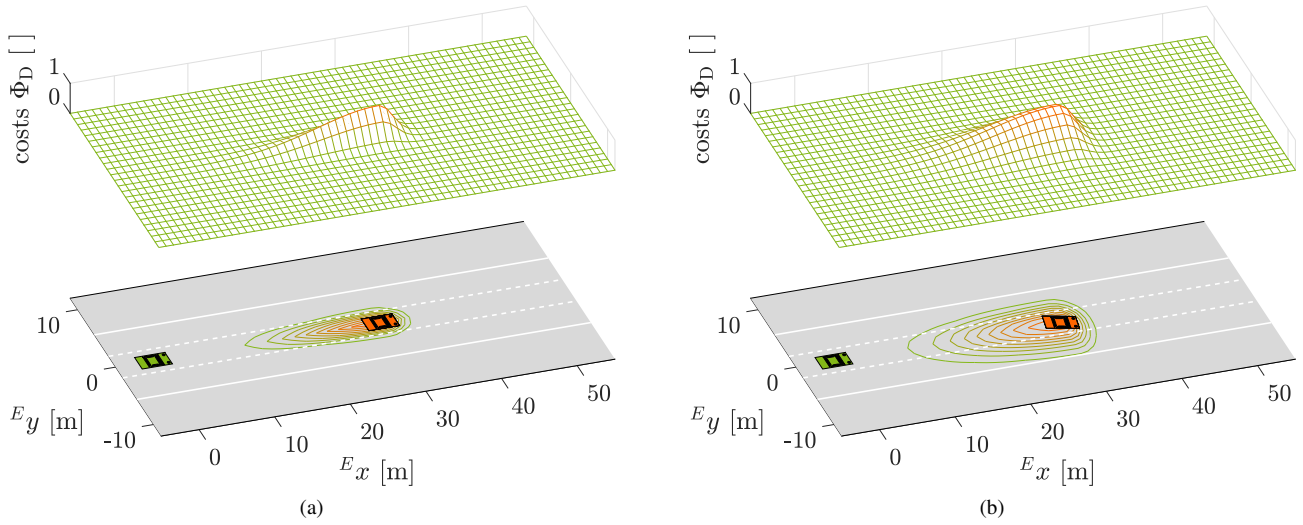

Fig. 3: Illustration of the dynamic potential field, denoting potential collision risk. The ego vehicle is driving at a speed of 120 km/h. The obstacle vehicle has a speed of 85 km/h with a heading angle of (a) ${}^F\lambda^{\varrho=1} = 0\,^\circ$ and (b) ${}^F\lambda^{\varrho=1} = -13\,^\circ$. The dynamic potential field is build for each predicted point in time, in order to take the predicted relative velocities at that time into account. Thus it is possible to predictively consider the situation dependent, varying safety distances.

B. Dynamic Environment Modeling

To take dynamic obstacles into account obstacles are predicted utilizing a lane change detection and the predicted time-to-lane-change t_{ttlc} [13] for trajectory prediction. In the following obstacle quantities are denoted with ϱ. For $\varrho = 1 \dots \rho$ obstacles the lateral and longitudinal distance between the ego and obstacle vehicle trajectory is calculated separately

$$\Delta x_k^\varrho = {}^F x_k - {}^F x_k^\varrho, \tag{15}$$

$$\Delta y_k^\varrho = {}^F y_k - {}^F y_k^\varrho. \tag{16}$$

For safety reasons the necessary distance to be satisfied is given by the approximation of braking distance

$$\Delta b^\varrho = \Delta v^{\varrho\,2}/(2a) \tag{17}$$

with parameter a for the maximum braking acceleration. However regarding equation (17) any other desired distance is possible. The relative velocity Δv^ϱ is calculated in longitudinal

$$\Delta v_{x,k}^\varrho = {}^F v_{x,k} - {}^F v_{x,k}^\varrho \tag{18}$$

and lateral direction

$$\Delta v_{y,k}^\varrho = {}^F v_{y,k} - {}^F v_{y,k}^\varrho. \tag{19}$$

In case of low relative velocities, it should apply that a longitudinal minimum distance $\check{\Lambda}_{lon}^\varrho$ and lateral minimum distance $\check{\Lambda}_{lat}^\varrho$ between the ego and obstacle vehicle, considering the spatial extend of the vehicles, is always satisfied. The measured heading ${}^F\lambda^\varrho$ of the respective obstacle vehicle is used to rotate the predefined minimum desired safety distance according to the current situation. This leads to

$$\Lambda_{lon}^\varrho = \max\{|\check{\Lambda}_{lon}^\varrho \cos({}^F\lambda^\varrho)|, |\check{\Lambda}_{lat}^\varrho \sin({}^F\lambda^\varrho)|\}, \tag{20}$$

$$\Lambda_{lat}^\varrho = \max\{|\check{\Lambda}_{lat}^\varrho \cos({}^F\lambda^\varrho)|, |\check{\Lambda}_{lon}^\varrho \sin({}^F\lambda^\varrho)|\}. \tag{21}$$

With equation (17) the safety distance σ^ϱ to each respective obstacle ϱ is calculated. For the direction dependent component of the dynamic environment model the algebraic sign is considered for longitudinal and lateral direction

$$\sigma_{lon}^\varrho = \begin{cases} \Lambda_{lon}^\varrho & \operatorname{sgn}(\Delta x_k^\varrho\, \Delta v_{x,k}^\varrho) > 0 \\ \max\{\Delta b_{lon}^\varrho, \Lambda_{lon}^\varrho\} & \text{otherwise} \end{cases}, \tag{22}$$

$$\sigma_{lat}^\varrho = \begin{cases} \Lambda_{lat}^\varrho & \operatorname{sgn}(\Delta y_k^\varrho\, \Delta v_{y,k}^\varrho) > 0 \\ \max\{\Delta b_{lat}^\varrho, \Lambda_{lat}^\varrho\} & \text{otherwise} \end{cases}, \tag{23}$$

Hence, in case the ego and obstacle vehicle are moving away from each other just the minimum distance $\Lambda_{lon/lat}^\varrho$ between both vehicles has to be satisfied. A Gaussian function is utilized to model the dynamic potential field by taking the actual distance and the desired safety distance into account. Thus the requirement of a differentiable environment model is inherently fulfilled

$$d_{lon}^\varrho = \mathrm{e}^{-0.5\left(\frac{\Delta x^\varrho}{\sigma_{lon}^\varrho}\right)^2}, \tag{24}$$

$$d_{lat}^\varrho = \mathrm{e}^{-0.5\left(\frac{\Delta y^\varrho}{\sigma_{lat}^\varrho}\right)^2}. \tag{25}$$

Based on the characteristics of the Gaussian function the combination of longitudinal and lateral potential costs yields

$$h_{\varrho,k} = d_{lon}^\varrho d_{lat}^\varrho. \tag{26}$$

Costs Φ_D representing the dynamic potential field are generated with vectorized $h_{\varrho,k}$ for each $\chi(\mathbf{h}_\varrho)$ analogous to the static potential field. The characteristic of the dynamic potential field with respect to a difference in orientation is shown in Fig. 3. On the basis of the relative velocity in longitudinal and lateral direction the safety distance is adapted.

C. Environment potential field

The resulting environment model is given by the superposition of the static and the dynamic potential field. The static potential field divides into negotiable and non-negotiable space based on the road geometry, whereas the dynamic potential field represents a potential collision risk with dynamic obstacles. In Fig. 4 the combination of the static potential field (cmp. Fig. 2) and the dynamic potential field with the obstacle vehicle aligned to the ego vehicle (cmp. Fig. 3(a)) is illustrated. As the static and the dynamic

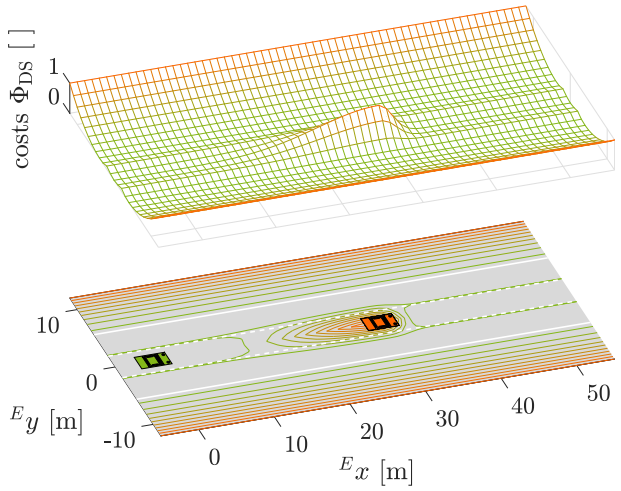

Fig. 4: Resulting environment potential field from superposition of the static and the dynamic potential field.

potential field both influence the resulting trajectory a compromise has to be found, balancing the realization of a lane keeping or lane change maneuver. This can be realized by choosing the parameters of the trajectory planning approach (e.g. weight matrix $\mathbf{\Omega}$) and parameters of the environment model (e.g. the desired distance to the respective lane marker Λ_ℓ and minimum safety distance $\check{\Lambda}^{\varrho}_{lon/lat}$) appropriately. Due to its characteristics the developed environment model can be described as a predictive environment potential field Φ_{DS}.

IV. Results

To show the general functioning of the developed algorithm simulations are performed with the help of a dynamic environment simulation developed by [17]. Therein camera and radar sensors are modeled in correspondence to a realistic view range and detection area. The simulated ego vehicle is equipped with radar sensors to the front, rear and sides and a front facing camera. Thus lane marker information and fused information about obstacle vehicles is provided. A reference position is generated by the trajectory planning approach and applied likewise receding horizon control. Results are shown for straight lanes, but the developed environment model also holds for curved road scenarios.

A. Simulation results

To illustrate the characteristics of the environment model in cooperation with the optimization-based trajectory planning approach a scenario is chosen, which consists of a highway segment with three lanes of 3.75 m width and two obstacle vehicles. The initial conditions at time $t = 0\,\mathrm{s}$ are shown in Tab. I. During simulation vehicle velocities may vary because of the implemented individual driving behavior of the traffic participants. Fig. 5 shows the results obtained

TABLE I: Start conditions of ego vehicle and obstacle vehicles in analyzed scenario.

	ID	$^E x$ [m]	$^E y$ [m]	$^F v$ [km/h]	$^F \lambda$ [°]
ego vehicle	0	0	-3.75	120	0
obstacle vehicle	1	60	-3.15	85	0.1
obstacle vehicle	2	90	-3.75	57.2	0

by the presented approach in steps of 1.5 s beginning at $t = 0.6\,\mathrm{s}$. At that time the ego vehicle and obstacle vehicle 1 are driving on the most right lane. The ego vehicle moves faster than obstacle vehicle 1 and the dynamic potential field is shaped in accordance to the relative speed of approximately $35\,\frac{\mathrm{km}}{\mathrm{h}}$. In the further course obstacle vehicle 1 is overtaking slower obstacle vehicle 2. With respect to the ego vehicle two dynamic potential fields superimpose. The safety distance is given in accordance to the relative speed, such that for obstacle vehicle 1 a smaller safety distance is valid than for obstacle vehicle 2. Like obstacle vehicle 1 the ego vehicle performs a lane change to the left to overtake obstacle vehicle 2. Supported by the predictive potential field the ego vehicle can immediately initiate an optimal subsequent maneuver. By performing a further lane change to the left the ego vehicle overtakes obstacle vehicle 1 maintaining the desired speed. Throughout the maneuver due to only small deviations in orientation the shape of the dynamic potential field is mainly oriented in longitudinal direction. The static potential field is foremost visible at the road boundaries. Nonetheless it is evident that the static field also enables precise lane keeping by considering the lane dimensions via the applied dashed lane marker model. The results depicted in Fig. 5 clearly show the dependence of the environment model on profound sensor data. Lane markers are only detected by the camera sensor, which could lead to a limited lane marker detection caused by occultation or a narrow sensor field of view. Within the environment model the view range of each lane marker is considered in a way that no costs are generated if the view range is exceeded. In future work problems arising from low view ranges can be solved by the inclusion of map data.

V. Conclusion

This contribution presents an approach to environment modeling for the use in optimization-based trajectory planning approaches. The environment model is represented as a potential field, which is composed of a static and a dynamic part. The dynamic part provides an interpretable model based on physical considerations taking the vehicle kinematics into account. The novelty, which separates the developed approach from others, lies in the fact that the environment potential field incorporates knowledge about the future development of the current situation by the use of trajectory planning and

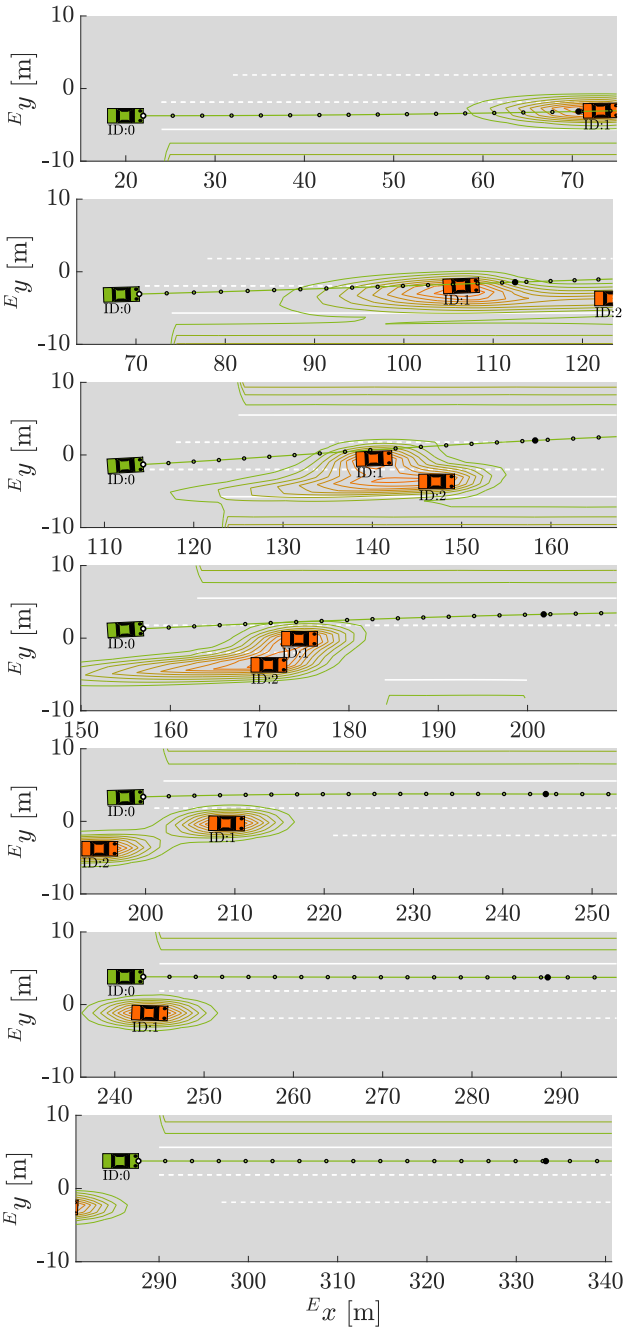

Fig. 5: For each time step the current situation is depicted with reference to the moving ego vehicle. In addition to the environment potential field the planned ego trajectory is visualized. Note: The ego trajectory intersecting with the potential field does not indicate a collision as the environment potential field is only shown for the current time step. However, based on the predicted situation the evolving potential field is directly incorporated into trajectory planning.

obstacle prediction, which simultaneously affect the safety distance that has to be satisfied. Without any regard to the developing situation a fixed, oversized safety distance will lead to unnecessarily high deceleration, whereas a predetermined, undersized safety distance will give rise to risky behavior. Due to its predictive manner the developed environment model significantly improves safety and comfort in complex traffic scenarios. The analysis shows that the developed environment model is unconditionally suitable for highway scenarios. Furthermore the environment model can easily be enhanced by a more sophisticated calculation of the braking distance to consider for example road conditions. In future work the complete environment model will be integrated in the test vehicle and tested in real traffic.

References

[1] B. Paden, M. Čáp, S. Z. Yong, D. Yershov, and E. Frazzoli, "A survey of motion planning and control techniques for self-driving urban vehicles," *IEEE Transactions on Intelligent Vehicles*, vol. 1, no. 1, pp. 33–55, 2016.

[2] C. Götte, M. Keller, T. Nattermann, C. Haß, K.-H. Glander, and T. Bertram, "Spline-based motion planning for automated driving," in *Proceedings of the 20th IFAC World Congress*, 2017, pp. 9444–9449.

[3] J. Ziegler, P. Bender, T. Dang, and C. Stiller, "Trajectory planning for bertha — a local, continuous method," in *IEEE Intelligent Vehicles Symposium (IV), 2014*, 2014, pp. 450–457.

[4] C. Götte, M. Keller, C. Rösmann, T. Nattermann, C. Haß, K.-H. Glander, A. Seewald, and T. Bertram, "A real-time capable model predictive approach to lateral vehicle guidance," in *IEEE International Conference on Intelligent Transportation Systems (ITSC), 2016*, 2016, pp. 1908–1913.

[5] J. Nilsson, P. Falcone, M. Ali, and J. Sjöberg, "Receding horizon maneuver generation for automated highway driving," *Control Engineering Practice*, vol. 41, pp. 124–133, 2015.

[6] A. Elfes, "Using occupancy grids for mobile robot perception and navigation," *Computer*, vol. 22, no. 6, pp. 46–57, 1989.

[7] G. Tanzmeister and D. Wollherr, "Evidential grid-based tracking and mapping," *IEEE Transactions on Intelligent Transportation Systems*, vol. 18, no. 6, pp. 1454–1467, 2017.

[8] H. Mouhagir, R. Talj, V. Cherfaoui, F. Aioun, and F. Guillemard, "Integrating safety distances with trajectory planning by modifying the occupancy grid for autonomous vehicle navigation," in *IEEE International Conference on Intelligent Transportation Systems (ITSC), 2016*, 2016, pp. 1114–1119.

[9] E. Bauer, F. Lotz, M. Pfromm, M. Schreier, B. Abendroth, S. Cieler, A. Eckert, A. Hohm, S. Lüke, P. Rieth, V. Willert, and J. Adamy, "Proreta 3: An integrated approach to collision avoidance and vehicle automation," *at - Automatisierungstechnik*, vol. 60, no. 12, pp. 755–765, 2012.

[10] J. Wang, J. Wu, and Y. Li, "The driving safety field based on driver–vehicle–road interactions," *IEEE Transactions on Intelligent Transportation Systems*, vol. 16, no. 4, pp. 2203–2214, 2015.

[11] T. Brandt, T. Sattel, and M. Böhm, "Combining haptic human-machine interaction with predictive path planning for lane-keeping and collision avoidance systems," in *IEEE Intelligent Vehicles Symposium (IV), 2007*, 2007, pp. 582–587.

[12] W. Burgard and M. Hebert, "World modeling," in *Springer Handbook of Robotics*, B. Siciliano and O. Khatib, Eds. Berlin, Heidelberg: Springer Berlin Heidelberg, 2008, pp. 853–869.

[13] C. Wissing, T. Nattermann, K.-H. Glander, and T. Bertram, "Probabilistic time-to-lane-change prediction on highways," in *IEEE Intelligent Vehicles Symposium (IV), 2017*, 2017, pp. 1452–1457.

[14] C. Rösmann, W. Feiten, T. Woesch, F. Hoffmann, and T. Bertram, "Trajectory modification considering dynamic constraints of autonomous robots," in *Proceedings of ROBOTIK 2012 - 7th German Conference on Robotics*, 2012, pp. 74–79.

[15] K. Levenberg, "A method for the solution of certain non-linear problems in least squares," *Quarterly of Applied Mathematics*, vol. 2, no. 2, pp. 164–168, 1944.

[16] D. W. Marquardt, "An algorithm for least-squares estimation of nonlinear parameters," *Journal of the Society for Industrial and Applied Mathematics*, vol. 11, no. 2, pp. 431–441, 1963.

[17] C. Wissing, T. Nattermann, K.-H. Glander, A. Seewald, and T. Bertram, "Environment simulation for the development, evaluation and verification of underlying algorithms for automated driving," in *AmE 2016 - Automotive meets Electronics; 7th GMM-Symposium*, 2016, pp. 9–14.